Biochemical and Biophysical Research Communications 424 (2012) 456–461

Contents lists available at SciVerse ScienceDirect

Biochemical and Biophysical Research Communications

journal homepage: www.elsevier.com/locate/ybbrc

CXCL2 synthesized by oral squamous cell carcinoma is involved in cancer-associated bone destruction

Erika Oue [a,b,c], Ji-Won Lee [a], Kei Sakamoto [a], Tadahiro Iimura [a,c], Kazuhiro Aoki [d], Kou Kayamori [e,f], Yasuyuki Michi [b], Masashi Yamashiro [b], Kiyoshi Harada [b], Teruo Amagasa [b], Akira Yamaguchi [a,c,*]

[a] Section of Oral Pathology, Graduate School of Medical and Dental Sciences, Tokyo Medical and Dental University, Japan
[b] Section of Maxillofacial Surgery, Graduate School of Medical and Dental Sciences, Tokyo Medical and Dental University, Japan
[c] Global Center of Excellence (GCOE) Program, International Research Center for Molecular Science in Tooth and Bone Diseases, Tokyo Medical and Dental University, Tokyo, Japan
[d] Section of Pharmacology, Graduate School of Medical and Dental Sciences, Tokyo Medical and Dental University, Japan
[e] Section of Diagnostic Oral Pathology, Graduate School of Medical and Dental Sciences, Tokyo Medical and Dental University, Japan
[f] Department of Pathology, Ome Municipal General Hospital, Ome, Tokyo, Japan

ARTICLE INFO

Article history:
Received 22 June 2012
Available online 4 July 2012

Keywords:
Oral cancer
CXCL2
Osteoclast
Bone resorption
RANKL

ABSTRACT

To explore the mechanism of bone destruction associated with oral cancer, we identified factors that stimulate osteoclastic bone resorption in oral squamous cell carcinoma. Two clonal cell lines, HSC3-C13 and HSC3-C17, were isolated from the maternal oral cancer cell line, HSC3. The conditioned medium from HSC3-C13 cells showed the highest induction of *Rankl* expression in the mouse stromal cell lines ST2 and UAMS-32 as compared to that in maternal HSC3 cells and HSC3-C17 cells, which showed similar activity. The conditioned medium from HSC3-C13 cells significantly increased the number of osteoclasts in a co-culture with mouse bone marrow cells and UAMS-32 cells. Xenograft tumors generated from these clonal cell lines into the periosteal region of the parietal bone in athymic mice showed that HSC3-C13 cells caused extensive bone destruction and a significant increase in osteoclast numbers as compared to HSC3-C17 cells. Gene expression was compared between HSC3-C13 and HSC3-C17 cells by using microarray analysis, which showed that *CXCL2* gene was highly expressed in HSC3-C13 cells as compared to HSC3-C17 cells. Immunohistochemical staining revealed the localization of CXCL2 in human oral squamous cell carcinomas. The increase in osteoclast numbers induced by the HSC3-C13-conditioned medium was dose-dependently inhibited by addition of anti-human CXCL2-neutralizing antibody in a co-culture system. Recombinant CXCL2 increased the expression of *Rankl* in UAMS-32 cells. These results indicate that CXCL2 is involved in bone destruction induced by oral cancer. This is the first report showing the role of CXCL2 in cancer-associated bone destruction.

1. Introduction

Cancer-associated bone destruction is caused by the direct invasion of cancer cells and metastasis of cancer cells into the bone. The former is frequently observed in oral cancers. Although the destruction of bone caused by invading oral cancer is associated with poor prognosis [1–3], the molecular mechanisms underlying this process are not well understood. We previously reported that fibroblastic stromal cells located at the interface between cancer and bone play critical roles in osteoclastic bone resorption by producing the receptor activator of NF-κB (RANK) ligand (RANKL) [4]. RANKL produced by stromal cells and osteoblastic cells binds to RANK expressed in osteoclast progenitors, which promotes osteoclastogenesis [5]. Thus, RANK–RANKL signaling plays an essential role in osteoclastogenesis [6].

Cancer-associated bone destruction is critically regulated by various factors synthesized by cancer cells, such as parathyroid hormone-related peptide (PTHrP), interleukin (IL)-6, IL-11, tumor necrosis factor-α (TNF-α), and prostaglandin E(2) [7–12], which are also synthesized by oral squamous cell carcinoma (OSCC) cells. These factors stimulate RANKL expression in stromal cells and osteoblastic cells adjacent to the resorbing bone. IL-6 produced by stromal cells in OSCC induces fibroblastic stromal cells to produce RANKL [12]. Although this cascade provides a new mechanism of osteoclastic bone resorption induced by OSCC, the induction of RANKL synthesis by cancer-derived factor(s) in stromal cells is not well understood. We therefore investigated the cancer-derived factors that regulate osteoclastic bone resorption by stimulating RANKL expression in stromal cells. For this purpose, we isolated clonal cancer cell lines from the maternal OSCC cell line HSC3 [13] and identified 2 clones that exhibited high (HSC3-C13)

* Corresponding author at: Section of Oral Pathology, Graduate School of Medical and Dental Sciences, Tokyo Medical and Dental University, 1-5-45 Yushima, Bunkyo-ku, Tokyo 113-8549, Japan. Fax: +81 3 5803 0188.
E-mail address: akira.mpa@tmd.ac.jp (A. Yamaguchi).

0006-291X/$ - see front matter © 2012 Elsevier Inc. All rights reserved.
http://dx.doi.org/10.1016/j.bbrc.2012.06.132

Table 1
Primer sequences of RT-PCR.

Gene	Forward	Reverse
Mouse *Rankl*	5′-ATGATGGAAGGCTCATGGT-3′	3′-CCAAGAGGACAGAGTGACTTT-5′
Mouse *Opg*	5′-CTGCCTGGGAAGAAGATCAG-3′	3′-TTGTGAAGCTGTGCAGGAAC-5′
Human *CXCL2*	5′-CTCAAGAATGGGCAGAAAGC-3′	3′-AAACACATTAGGCGCAATCC-5′
18SrRNA	5′-GTAACCCGTTGAACCCCATT-3′	3′-CCATCCAATCGGTAGTAGCG-5′

and low (HSC3-C17) activities to induce *Rankl* expression in stromal cells. The gene expression differences between these clonal cell lines were investigated using microarray analysis, which identified *CXCL2* as a candidate gene that effectively induces *RANKL* expression in stromal cells.

CXCL2 is a chemokine produced by endotoxin-treated macrophages and plays an important role as a mediator of inflammation [14,15]. Ha et al. first reported that CXCL2 is involved in osteoclastic bone resorption and suggested its participation in inflammatory bone destructive diseases [16,17]. Recently, Dong et al. reported that serum levels of CXCL2, also known as GROβ (growth-related gene product β), in esophageal squamous cell carcinoma patients were much higher than that in healthy controls [18]. They also showed that CXCL2 and its downstream effector early growth response protein (EGR1) is involved in cisplatin-induced apoptosis in a human esophageal squamous cell carcinoma cell line [19]. However, little is know about the roles of CXCL2 in bone destruction induced by OSCC. Here, we demonstrate for the first time that CXCL2 plays a role in bone destruction associated with OSCC.

2. Materials and methods

2.1. Reagents

Rabbit anti-human CXCL2-neutralizing polyclonal antibody was purchased from Abcam Inc. (Cambridge, UK). Rabbit anti GRO-beta MIP2-alpha polyclonal antibody (ABBIOTEC, San Diego, CA) was used to detect human CXCL2 by immunohistochemistry. Recombinant human GRO beta (CXCL2) was purchased from PeproTecj Inc. (Rocky Hill, NJ). All other chemicals and reagents were of analytical grade.

2.2. Cell culture

The human OSCC cell lines, Ca9-22, Ho-1-N-1, HSC-3, and SKN-3, were purchased from the Japanese Collection of Research Bioresources (JCRD, Osaka, Japan). All cell lines were maintained in Dulbecco's modified Eagle's medium containing 10% fetal bovine serum (FBS) (Sigma–Aldrich, St. Louis, MO), 50-units/ml penicillin G, and 50-mg/ml streptomycin. Single-cell derived clonal cell lines were isolated from HSC3 cells by using the limiting dilution technique with 96-well plates. All the 96-well plates were examined using microscope, and wells containing only 1 cell on the day after inoculation were selected. These wells were further incubated for 3 weeks, and the cells in each well were expanded separately. The stromal cell line ST2, derived from mouse bone marrow, was purchased from RIKEN BioResource Center (Tsukuba, Japan). Mouse osteoblastic UAMS-32 cells were provided by Dr. O'Brien [14]. ST2 cells were maintained in RPMI 1640 medium containing 10% FBS. UAMS-32 cells were cultured in α-minimum essential medium (α-MEM) containing 10% FBS. To assess the effect of recombinant CXCL2 on *Rankl* and *Opg* expression in UAMS-32 cells, the cells were treated for 42 h with various concentrations of recombinant CXCL2.

To collect conditioned medium, the maternal HSC3 cells, HSC3-C13 cells, and HSC3-C17 cells were grown to confluence in 100-mm dishes in Dulbecco's modified Eagle's medium containing 10% FBS. After washing 3 times with PBS, the cells were cultured for an additional 48 h in 4-ml serum-free α-MEM. The collected culture supernatants were centrifuged at 1500 rpm for 5 min and filtered using a 0.22-μm filter unit. The media thus obtained were stored at −80 °C and used as conditioned medium by appropriate dilution with serum-free α-MEM.

2.3. Reverse transcriptase-PCR analysis

Reverse transcriptase-PCR (RT-PCR) analysis was performed using total RNA extracted from the cultured cells with NucleoSpin (Macherey–Nagel, Duren, Germany). RNA aliquots were reverse transcribed to complementary DNAs by using an oligo (dT) primer (Roche), deoxynucleotide triphosphate (dNTP; Promega), and Moloney murine leukemia virus (M-MuLV) reverse transcriptase (Fermentas, Hanover, MD). The complementary DNA products were PCR amplified using gene-specific primers for mouse *Rankl*, *Opg*, and human *CXCL2* (Table 1). Real-time RT-PCR was performed using a LightCycler System (Roche) with a Platinum SYBR Green qPCR SuperMix UDG kit (Invitrogen, Carlsbad, CA). The relative amount of each mRNA in each sample was normalized to the 18S rRNA level.

2.4. Microarray analysis

Two clonal cell lines (HSC3-C13 and HSC3-C17) were used for microarray analysis with the Affymetrix Human Genome U133 Plus 2.0 arrays. Labeling, hybridization, and staining were performed according to the manufacturer's protocol by using total RNA as the starting material. The arrays were scanned using the GeneArray Scanner (Affymetrix), and the data were preprocessed using the GeneChip Operating Software (Affymetrix) according to the manufacturer's default parameters.

2.5. Osteoclast formation

Bone marrow cells (BMCs) were obtained from the tibiae of 4–6-week-old ddY male mice. BMCs (2.5×10^7 cells/well) were co-cultured with UASM-32 cells (2.5×10^6 cells/well) on 24-well plates in the presence of CM for 5 days. After fixing the co-cultured cells in 10% buffered formalin, the cells were stained with tartrate-resistant acid phosphatase (TRAP) for osteoclast identification by incubating with 0.1-mol/L sodium acetate buffer (pH 5.0) containing AS-MX phosphate (Sigma–Aldrich) and red violet LB salt (Sigma–Aldrich) in the presence of 50-mmol/L sodium tartrate (Sigma–Aldrich). TRAP-positive cells that contained more than 3 nuclei were identified as osteoclasts and were counted. In some experiments, the effects of anti-human CXCL2-neutralizing antibody on osteoclast formation were tested.

2.6. HSC3 cell xenograft implantation into athymic mice

HSC3-C13 and HSC3-C17 cells (5×10^5 cells/injection) were injected in the periosteal region of the parietal bones of athymic mice by using a 1-ml syringe after scratching the periosteum once with the syringe needle [12]. Three weeks after the transplantation, the

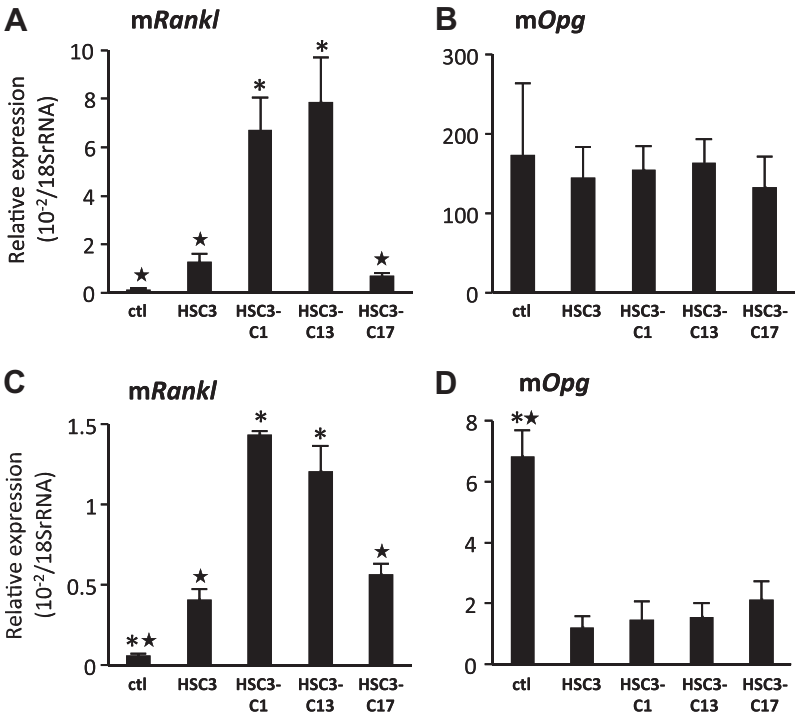

Fig. 1. Effect of conditioned media (CM) collected from maternal HSC3, HSC3-C13, and HSC3-C17 cells on the expression of *Rankl* (A, C) and *Opg* (B, D) in ST2 cells (A, B) and UASM-32 cells (C, D). After 24 h, each CM was added to the culture and maintained for 72 h. Each CM was diluted to 1:1 with serum-free α-MEM. Ctl: control culture without CM supplementation. $^{*}p < 0.05$, significantly different from the value of the maternal HSC3. $^{\star}p < 0.05$, significantly different from the value of HSC3-C13 cells.

calvarial region was dissected and fixed with 4% paraformaldehyde. Soft radiographic images were obtained after fixation. Microtomography images were scanned at 30 μm by using microcomputer tomography imaging system (smx100ct, Shimadzu, Kyoto, Japan). The tissues were embedded in paraffin after decalcification with 10% EDTA at 4 °C for 10 days. The experimental procedures were reviewed and approved by the Animal Care and Use Committees at Tokyo Medical and Dental University.

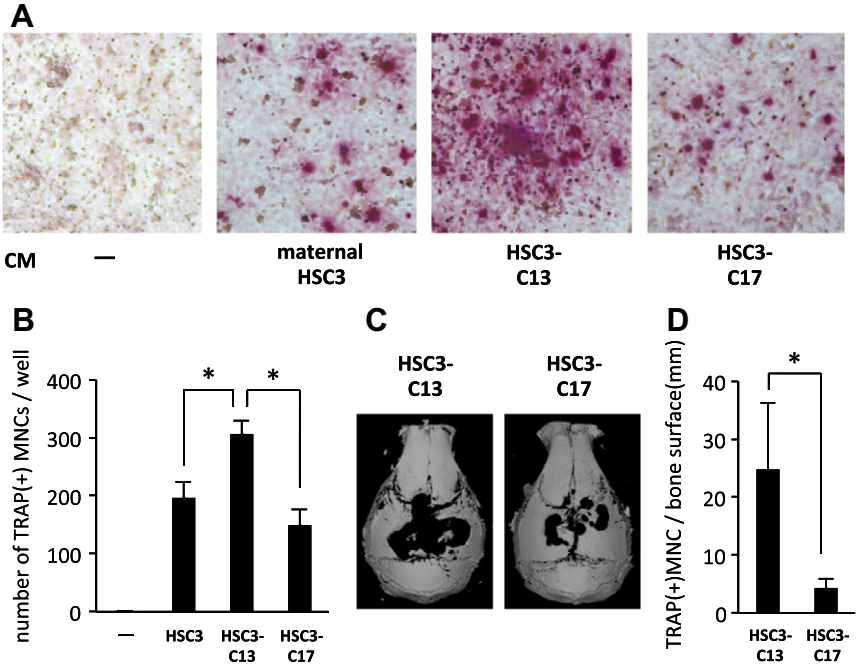

Fig. 2. Effects of CM from maternal HSC3, HSC3-C13, and HSC3-C17 cells on osteoclast formation in a co-culture system. One day after the inoculation of bone marrow cells and UAMS-32 cells, CM from each cell line (3:7 dilution with serum-free α-MEM) was added into the culture and maintained for 5 days. Typical features of a TRAP-stained well (A) and the number of osteoclasts in each group (B). Bone-resorbing activities of HSC3-C13 and HSC3-C17 cells in xenograft experiments (C and D). (C) Microtomography images of HSC3-C13 and HSC3-C17 cells after 3 weeks of the transplantation into the periosteal region of the parietal bone of athymic mice. D: the number of TRAP-positive osteoclasts assessed by TRAP-stained sections. $^{*}p < 0.05$, significantly different from the value of the maternal HSC3.

2.7. Immunohistochemical localization of CXCL2 in human cases of OSCC

After fixation in 10% neutral buffered formalin, small blocks containing the interface of tumor and bone were dissected from 6 of the surgical cases. These specimens were decalcified in 10% EDTA at 4 °C for 4 weeks and embedded in paraffin. For immunohistochemical staining, the sections were pretreated with microwave irradiation in 0.01 M citric acid for 1 h at 80 °C. After quenching endogenous peroxidase activity by incubation in 3% hydrogen peroxide solution for 20 min, the sections were incubated overnight at 4 °C with rabbit anti-GRO-beta MIP2-alpha polyclonal antibody (1:50) to detect immuno-localization of CXCL2. The sections were incubated with peroxidase-conjugated secondary antibody (Envision + Dual Link System Peroxidase Kit; Dako) for 1 h. Diaminobenzidine was used as a chromogen.

2.8. Statistical analyses

We used analysis of variance with an *F*-test, followed by a *t*-test. *p*-Values less than 0.05 were considered significant. The data are presented as mean ± standard deviation of independent replicates.

3. Results

3.1. Single cell-derived clonal cell lines isolated from HSC3 cells exhibited different Rankl-inducing effects on mouse stromal cells

We isolated 20 single cell-derived clones from the maternal HSC3 cells, of which 13 successfully retained the proliferative capacity despite several passages. The effect of the CM collected from these 13 clones on the expression of *Rankl* and *Opg* mRNAs was assessed using a mouse stromal cell line, ST2. Of these clones, the CM from HSC3-C1 cells and HSC3-C13 cells had the highest *Rankl*-inducing effect on ST2 cells, while the CM from HSC3-C17 cells showed the lowest *Rankl* induction (Fig. 1A). There were no significant differences in the effects of these CMs on the induction of *Opg* expression in ST2 cells (Fig. 1B). To confirm the *Rankl*- and *Opg*-inducing activities, the effects of CMs from HSC3-C1, HSC3-C13, and HSC3-C17 cells on *Rankl* and *Opg* expression were assessed using a different mouse osteoblastic cell line, UAMS-32. As shown in Fig. 1C, CMs from HSC3-C1 and HSC3-C13 cells induced a high level of *Rankl* expression as compared to the CM from the maternal HSC3 cells. The CM from HSC3-C17 cells did not differ from that of the maternal HSC3 cells and had significantly lower effect than that the CM of HSC3-C13 on the induction of *Rankl* expression in UAMS-32 cells. The CMs from the maternal HSC3 cells, HSC3-C1 cells, HSC3-C13 cells, and HSC3-C17 cells showed no significant differences in the effects of these CMs on the induction of *Opg* expression, while *Opg* expression in these cultures exhibited lower levels than that in the culture without CM supplementation. Based on these experiments, HSC3-C13 cells were selected as high *Rankl*-inducing cells and HSC3-C17 as low *Rankl*-inducing cells in subsequent experiments.

3.2. CM from HSC3-C13 cells more effectively induced osteoclastogenesis than that from HSC3-C17 cells

We investigated the effects of CMs from the maternal HSC3 cells, HSC3-C13 cells, and HSC3-C17 cells on osteoclast formation by using a mouse co-culture system. The number of TRAP-positive osteoclastic cells increased in the presence of the CMs from all the tested cell lines as compared to the culture without CM supplementation, and CM from CH3-C13 cells most effectively induced the formation of TRAP-positive osteoclastic cells (Fig. 2A). Fig. 2B summarizes the quantitative data for the number of TRAP-positive osteoclastic cells induced by addition of each CM. The induction of TRAP-positive cells was significantly higher in the presence of HSC3-C13 CM than in the presence of HSC3-C17 CM, while the inducing effect of HSC3-C17 cells did not differ significantly from that of the maternal HSC3 cells. These results indicate that CM from HSC3-C13 cells contained higher amounts of soluble factors capable of stimulating osteoclastogenesis than that from HSC3-C17 cells.

3.3. HSC3-C13 cells induced more extensive bone resorption than HSC3-C17 cells

The ability of these cell lines to induce bone resorption was examined by transplanting HSC3-C13 and HSC3-C17 cells into the calvarial region of athymic mice. Microcomputer tomography analysis showed that HSC3-C13 cells caused extensive bone resorption in mouse calvariae as compared to HSC3-C17 cells (Fig. 2C). Histological examinations showed that HSC3-C13 cell transplantation was associated with a significant increase in the number of TRAP-positive osteoclasts in the bone resorbing area as compared to HSC3-C17 cells (Fig. 2D).

3.4. Microarray analysis shows that CXCL2 is highly expressed in HSC3-C13 cells

The results of *in vitro* and *in vivo* experiments showed that HSC3-C13 and HSC3-C17 cells induce osteoclast differentiation and function with different potencies, suggesting that HSC3-C13 cells might synthesize an increased amount of soluble factors capable of regulating osteoclast differentiation as compared to HSC3-C17 cells. To identify these factors, HSC3-C13 and HSC3-C17 cells were subjected to microarray analysis, which showed different gene expression profiles. We then selected genes that exhibited 5 times higher expression levels in HSC3-C13 cells as compared to that in HSC3-C17 cells and found 11 genes (Table 2); of these, we focused on *CXCL2* as a target for further study based on the importance of chemokines in osteoclastic bone resorption.

3.5. Expression of CXCL2 in OSCC

To validate the results of microarray analysis, we investigated *CXCL2* expression in the maternal HSC3, HSC3-C13, and HSC3-C17 cells by using real-time RT-PCR. We confirmed that the level of *CXCL2* mRNA expression in HSC3-C13 cells was significantly higher than that in the maternal HSC3 cells and HSC3-C17 cells (Fig. 3A). HSC3-C13 cells showed an approximately 12-fold

Table 2
Genes that exhibited 5 times higher expression levels in HSC3-C13 cells as compared to that in HSC3-C17 cells.

Gene symbol	Gene name	Fold change clone 13/clone 17
IL6	Interleukin 6	25.99
MFAP5	Microfibrillar associated protein 5	22.63
PDZK1IP1	PDZK1 interacting protein 1	10.56
FAM155A	Family with sequence similarity 155, member A	9.19
PTGS2	Prostaglandin endoperoxide synthase 2	8.57
CXCL2	Chemokine (C–X–C motif) ligand 2	7.46
AKAP12	A kinase (PRKA) anchor protein 12	6.96
DUSP1	Dual specificity phosphatase 1	6.50
NEK3	NIMA (never in mitosis gene a)-related kinase 3	6.06
PLXNC1	Plexin C1	5.66
SAMD4A	Sterile alpha motif domain containing 4A	5.28

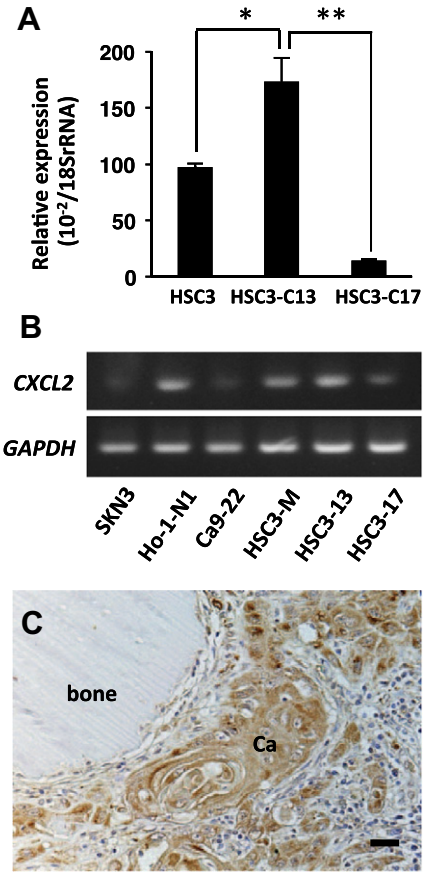

Fig. 3. Expression of CXCL2 in OSCC. (A) Expression levels of *CXCL2* in maternal HSC3, HSC3-C13, and HSC3-C17 cells, determined by RT-PCR analysis. $^{*}p < 0.05$, significantly different from the value of the maternal HSC3. $^{**}p < 0.01$, significantly different from the value of the maternal HSC3. (B) Expression of *CXCL2* mRNA in various OSCC cell lines. (C) Immunohistochemical localization of CXCL2 in a human OSCC case. Ca: cancer nest. Bar represent 20 μm.

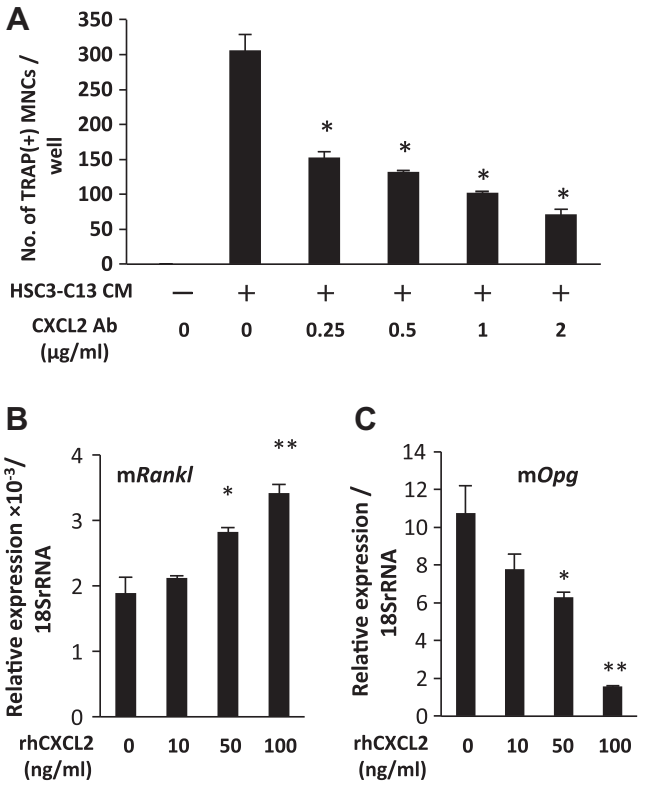

Fig. 4. (A) The effects of anti-human CXCL2-neutralizing antibody on formation of TRAP-positive osteoclastic cells. Co-culture with mouse bone marrow cells and UAMS-32 cell was performed in 24-well plates by using the same method used in Fig. 2. One day after the inoculation, CM from HSC3-C13 cells was added into the culture with or without various concentrations of anti-human CXCL2-neutralizing antibody and maintained for 5 days. $^{*}p < 0.05$, significantly different from the value of the cells treated with CM from HSC3-C13 without addition of anti-human CXCL2-neutralizing antibody. (B, C) The effects of recombinant CXCL2 on the expression levels of *Rankl* and *Opg* in UASM-32 cells. The cells were cultured with the indicated concentrations of recombinant CXCL2 for 5 days, and the expression levels of *Rankl* and *Opg* were determined by real time RT-PCR. $^{*}p < 0.05$, $^{**}p < 0.01$, significantly different from the value of the cells treated without addition of recombinant CXCL2.

increase in *CXCL2* mRNA levels as compared to HSC3-C17 cells (Fig. 3A). We also investigated *CXCL2* expression in other OSCC cell lines by RT-PCR (Fig. 3B). Ho-1-N1 cells showed high levels of *CXCL2* expression as well as HSC-C13 cells, while SKN3 and Ca9–22 cells showed lower levels of CXCl2 mRNA than that in HSC-C17 cells (Fig. 3B). To verify the expression of CXCL2 in human OSCC cases, we conducted the immunohistochemical staining for CXCL2 using paraffin sections obtained from surgical materials at mandibular resections. As shown in Fig. 3C, numerous SCCC cells showed positive signals for CXCL2, and a few inflammatory cells showed positive signals (Fig. 3C).

3.6. CXCL2 synthesized by cancer cells is involved in osteoclast formation

Next, the effects of neutralizing antibodies against human CXCL2 on osteoclastogenesis were examined using CM obtained from HSC3-C13 cells. Anti-human CXCL2 antibodies significantly inhibited HSC3-C13 CM-induced osteoclast formation in a dose-dependent manner (Fig. 4A), indicating that CXCL2 may be an important factor in osteoclast formation induced by HSC3-C13 cells.

3.7. CXCL2 stimulates Rankl expression and inhibits and Opg expression in UAMS-32 cells

We next investigated the effects of recombinant CXCL2 on the expression of *Rankl* and *Opg* in UAMS-32 cells. Recombinant CXCL2 significantly stimulated the expression of *Rankl* over the concentrations of 50 ng/ml, and simultaneously inhibited *Opg* expression at same concentrations (Fig. 4B, C). These results suggested that CXCL2 regulates osteoclastogenesis by controlling the expression levels of *Rankl* and *Opg*, respectively, in stromal/osteoblastic cells.

4. Discussion

In the present study, we investigated cancer-derived factors associated with the induction of osteoclastic bone resorption. To identify these factors, we isolated 13 clonal cell lines from the maternal OSCC cell line, HSC3. Of these, 2 clones (HSC3-C1 and HSC3-C13) showed extremely high *Rankl* expression-inducing effect on the 2 stromal cells lines, ST2 and UAMS-32, as compared to the maternal HSC3 cells. In contrast, HSC3-C17 cells showed the lowest activity to induce *Rankl* expression in these stromal cells, which activity was almost same as the maternal HSC3 cells. Thus we applied HSC3-C13 and HSC3–17 cells to microarray analysis to identify potential *Rankl*-inducing factor(s) preferentially expressed in HSC3–13 cells. We identified 11 genes showing 5 times higher levels in HSC3-C13 cells than in HSC3-C17 cells. In this assay, the gene showing the greatest expression difference between HSC3-C13 and HSC3-C17 cells was *IL-6*. Although *IL-6* expression varies among OSCC cell lines, we reported the HSC3 cell line express high levels of *IL-6* [12]. Moreover, IL-6 is a critical cytokine

involved in OSCC-related bone destruction [7,9,11,12]. These results support the validity of our microarray analysis.

We have previously reported that different OSCC cell lines have different *Rankl*-inducing effects on ST2 cells, with HSC3 cells showing 9 times higher activity than Ca9–22 and HO1-u-1 cells [12]. Although these results suggested that HSC3 cells and Ca9–22 or HO1-u-1 cells should be evaluated using microarray analysis to identify *Rankl*-inducing factors, the different genetic backgrounds of these cells could have resulted in extremely large differences in gene expression. Therefore, we isolated different clonal cell lines derived from HSC3 cells [13], which retain the same OSCC genetic background, showing high and low *Rankl*-inducing effects on ST2 cells. This strategy might be effective for obtaining the minimum number of differently expressed genes between the 2 clones by microarray analysis.

Ha et al. reported that RANKL induced bone marrow-derived macrophages to express CXCL2 through the JNK and NFκB signaling pathways, and this chemokine stimulated the proliferation of osteoclast precursors and increased osteoclast formation by promoting the migration and adhesion of osteoclasts [16,17]. These results indicate that RANKL is an upstream factor regulating CXCL2 expression. In the present study, we showed that recombinant CXCL2 stimulated *Rankl* expression in UAMS-32 osteoblastic cells, and the formation of TRAP-positive osteoclastic cells induced by CMs from HSC3-C13 cells was inhibited by CXCL2 neutralizing antibody. These findings suggest that CXCL2 synthesized by OSCC is involved in osteoclast formation by stimulating RANKL expression in stromal cells. Taken together, it is likely that a mutual paracrine loop between CXCL2 and RANKL is present during osteoclastogenesis; RANKL synthesized by bone marrow stromal cells could induce CXCL2 expression in bone marrow-derived macrophages, and CXCL2 produced by macrophages may stimulate RANKL expression in bone marrow stromal cells. During cancer-associated bone destruction, CXCL2 synthesized by cancer cells might participate in this paracrine loop by regulating RANKL expression. Since we also showed that CXCL2 inhibited *Opg* expression in stromal cells, CXCL2 might exert bi-functional action on osteoclastic bone formation by stimulating RANKL and inhibiting OPG.

Although the role of CXCL2 in the behavior of OSCC cells has not yet been well documented, Dong et al. reported that the serum levels of growth-related product β (GROβ), which is the alternative name of CXCL2, were much higher in esophagus squamous cell carcinoma patients than in healthy controls and suggested a role for CXCL2 in tumorigenesis and metastasis [18]. Based on a recent study by Yamada et al. [20] showing that RANKL produced by OSCC cells promotes epithelial mesenchymal transition and tumor progression, the paracrine loop between CXCL2 and RANKL may be involved in OSCC behavior, including cancer-associated bone resorption. Further investigation into the roles of CXCL2 in OSCC tumorigenesis and invasion will be important to understand the molecular mechanism underlying OSCC-associated bone destruction. The findings of these studies are expected to provide important information for the development of a new therapeutic approach to prevent cancer-associated bone destruction.

Acknowledgments

Grant-in-Aid for Scientific Research from the Japan Society for the Promotion of Science (Nos. 22249061, 21659420, and 23659854) and Health and Labour Sciences Research Grants from the Ministry of Health, Labour, and Welfare (No. 21040101) to A.Y., and by the Global Center of Excellence (GCOE) Program; International Research Center for Molecular Science in Tooth and Bone Diseases, Tokyo Medical and Dental University.

References

[1] I. Semba, H. Matsuuchi, Y. Miura, Histomorphometric analysis of osteoclastic resorption in bone directly invaded by gingival squamous cell carcinoma, J. Oral Pathol. Med. 25 (1996) 429–435.
[2] J.S. Brown, D. Lowe, N. Kalavrezos, J. D'Souza, P. Magennis, J. Woolgar, Patterns of invasion and routes of tumor entry into the mandible by oral squamous cell carcinoma, Head Neck 24 (2002) 370–383.
[3] R.J. Shaw, J.S. Brown, J.A. Woolgar, D. Lowe, S.N. Rogers, E.D. Vaughan, The influence of the pattern of mandibular invasion on recurrence and survival in oral squamous cell carcinoma, Head Neck 26 (2004) 861–869.
[4] M. Ishikuro, K. Sakamoto, K. Kayamori, T. Akashi, H. Kanda, T. Izumo, A. Yamaguchi, Significance of the fibrous stroma in bone invasion by human gingival squamous cell carcinomas, Bone 43 (2008) 621–627.
[5] H. Yasuda, N. Shima, N. Nakagawa, K. Yamaguchi, M. Kinosaki, S. Mochizuki, A. Tomoyasu, K. Yano, M. Goto, A. Murakami, E. Tsuda, T. Morinaga, K. Higashio, N. Udagawa, N. Takahashi, T. Suda, Osteoclast differentiation factor is a ligand for osteoprotegerin/osteoclastogenesis inhibitory factor and is identical to TRANCE/RANKL, Proc. Natl. Acad. Sci. 95 (1998) 3597–3602.
[6] B.F. Boyce, L. Xing, Functions of RANKL/RANK/OPG in bone modeling and remodeling, Arch. Biochem. Biophys. 473 (2008) 139–146.
[7] M. Okamoto, K. Hiura, G. Ohe, Y. Ohba, K. Terai, T. Oshikawa, S. Furuichi, H. Nishikawa, K. Moriyama, H. Yoshida, M. Sato, Mechanism for bone invasion of oral cancer cells mediated by interleukin-6 in vitro and in vivo, Cancer 89 (2000) 1966–1975.
[8] T. Tada, E. Jimi, M. Okamoto, S. Ozeki, K. Okabe, Oral squamous cell carcinoma cells induce osteoclast differentiation by suppression of os-teoprotegerin expression in osteoblasts, Int. J. Cancer 116 (2005) 253–262.
[9] T. Shibahara, T. Nomura, N. Cui, H. Noma, A study of osteoclast-related cytokines in mandibular invasion by squamous cell carcinoma, Int. J. Oral Maxillofac. Surg. 34 (2005) 789–793.
[10] K. Ono, T. Akatsu, N. Kugai, C.C. Pilbeam, L.G. Raisz, The effect of deletion of cyclooxygenase-2, prostaglandin receptor EP2, or EP4 in bone marrow cells on osteoclasts induced by mouse mammary cancer cell lines1, Bone 33 (2003) 798–804.
[11] E. Jimi, H. Furuta, K. Matsuo, K. Tominaga, T. Takahashi, O. Nakanishi, The cellular and molecular mechanisms of bone invasion by oral squamous cell carcinoma, Oral Dis. 17 (2011) 462–468.
[12] K. Kayamori, K. Sakamoto, T. Nakashima, H. Takayanagi, K. Morita, K. Omura, S.T. Nguyen, et al., Roles of interleukin-6 and parathyroid hormone-related peptide in osteoclast formation associated with oral cancers: significance of interleukin-6 synthesized by stromal cells in response to cancer cells, Am. J. Pathol. 176 (2010) 968–980.
[13] F. Momose, T. Araida, A. Negishi, H. Ichijo, S. Shioda, S. Sasaki, Variant sublines with different metastatic potentials selected in nude mice from human oral squamous cell carcinomas, J. Oral Pathol. Med. 18 (1989) 391–395.
[14] X. Li, D. Klintman, Q. Liu, T. Sato, B. Jeppsson, H. Thorlacius, Critical role of CXC chemokines in endotoxemic liver injury in mice, J. Leukoc. Biol. 75 (2004) 443–452.
[15] X. Ren, A. Carpenter, C. Hogaboam, L. Colletti, Mitogenic properties of endogenous and pharmacological doses of macrophage inflammatory protein-2 after 70% hepatectomy in the mouse, Am. J. Pathol. 163 (2003) 563–570.
[16] J. Ha, H. Choi, Y. Lee, H. Kwon, Y.W. Song, H. Kim, CXC chemokine ligand 2 induced by receptor activator of NF-kappa B ligand enhances osteoclastogenesis, J. Immunol. 184 (2010) 4717–4724.
[17] J. Ha, Y. Lee, H. Kim, CXCL2 mediates lipopolysaccharide-induced osteoclastogenesis in RANKL-primed precursors, Cytokine 55 (2011) 48–55.
[18] Q. Dong, J. Zhang, Q. Li, J.C. Bracher, D.T. Hendricks, X. Zhao, Clinical significance of serum expression of GROβ in esophageal squamous cell carcinoma, World J. Gastroenterol. 17 (2011) 2658–2662.
[19] Q. Dong, J. Zhang, D.T. Hendricks, X. Zhao, GROβ and its downstream effector EGR1 regulate cisplatin-induced apoptosis in WHCO1 cells, Oncol. Rep. 25 (2011) 1031–1037.
[20] T. Yamada, M. Tsuda, T. Takahashi, Y. Totsuka, M. Shindoh, Y. Ohba, RANKL expression specifically observed in vivo promotes epithelial mesenchymal transition and tumor progression, Am. J. Pathol. 178 (2011) 2845–2856.